

MAGNETIC PROPERTIES OF ROCKS FROM THE MOUNT ISA AREA

D.A. CLARK

CSIRO Division of Mineral Physics

PO Box 136

North Ryde, NSW

Australia 2113

JULY 1980

TABLE OF CONTENTS

	Page
1. INTRODUCTION	1
2. FIELD WORK	1
3. LABORATORY PROCEDURES	1
4. REMANENCE AND SUSCEPTIBILITY DATA	2
4.1 Sites 1-10	2
4.2 Sites 11-17	3
4.3 ECV Surface Samples	3
4.4 Sites 18-19	6
4.5 Urquhart Shale	6
5. MAGNETIC FABRIC	7
6. CONCLUSIONS	10

LIST OF TABLES

Table 1. Sampling Localities
Table 2. Susceptibility and Lineament Intensity Data
Table 3. Remanence Directions
Table 4. Magnetic Fabric

LIST OF FIGURES

Figure 1. Low-field susceptibility - temperature curves for specimens of Eastern Creek Volcanics.

Figure 2. Equal angle stereographic plots of directions of magnetisation measured from sites EV1-7 in the Eastern Creek Volcanics (the section beginning at Breakaway Creek to the east of the Microwave tower). A - NRM directions with respect to the present horizontal; the distribution is essentially planar between a normal and reversed direction. B - Magnetic cleaning (AF) reduces the scatter and two oppositely polarised groups of directions are revealed. The primitive represents to present horizontal.

Full (open) circles represent downward (upward) pointing directions.

Figure 3. Specimen directions, w.r.t. the present horizontal, after thermal treatment to 650°C for the Urquhart Shale.

Full (open) circles represent downward (upward) pointing directions.

1. INTRODUCTION

In February 1980 Mt Isa Mines Ltd initiated a proposal for an investigation by the CSIRO of the magnetic properties of rocks in the Mt Isa area in order to constrain and guide magnetic interpretation. Of particular interest was the variability of magnetisation of the Eastern Creek Volcanics, which form the magnetic basement in the mine area, and the origin of the various remanence components. A major aim was to assess the contribution of remanence to the observed magnetic anomalies.

2. FIELD WORK

Sampling was carried out by the CSIRO over three days in mid-March. Fifty underground and surface samples were collected and details of the sampling are given in Table 1. All surface samples were oriented using both magnetic and sun-compass bearings, but only magnetic bearings could be taken underground and the orientation of samples from the mine was therefore corrected for local declination values.

163 samples of the Eastern Creek Volcanics and 26 samples of the Urquhart Shale had been collected by the CSIRO in 1974 and 1975. The palaeomagnetic data, and much of the collected material, were made available and information from these sampling programmes has been incorporated into this report.

The Urquhart Shale was sampled throughout the succession exposed along a road under the railway bridge north of the mine. The ECVs were sampled in roadcuts and creek beds along the Cloncurry road from east of the microwave tower to Breakaway Creek, along the Gunpowder-Mt Isa road, through the type-section in Eastern Creek, and along the Julius Dam pipeline service road to the north of Mt Isa.

3. LABORATORY PROCEDURES

Susceptibilities were measured with a low frequency (211 Hz) transformer bridge developed by the CSIRO which is absolutely calibrated to

within one per cent. Remanence measurements were made with a Digico balanced fluxgate spinner magnetometer and susceptibility anisotropy by a Digico anisotropy spinner.

Curie point determinations for identification of magnetic minerals were made with the CSIRO susceptibility bridge equipped with a small furnace for heating a sample as its susceptibility is monitored.

Data on susceptibilities and remanent intensities of the samples are given in Table 2, remanence directions are summarised in Table 3 and magnetic fabric data, based on susceptibility anisotropy measurements, are listed in Table 4.

4. SUSCEPTIBILITY AND REMANENCE DATA

4.1 Sites 1-10

Although a traverse with an Elliott susceptibility meter had revealed moderate to high susceptibilities of the ECVs in this section of the cross-cut, most of the samples collected are relatively non-magnetic. From Table 2 it can be seen that except for two samples (MI4B and MI8) emu susceptibilities are less than 100×10^{-6} . In all cases Koenigsberger ratios are much less than unity, so remanence does not make a significant contribution to the anomaly associated with these rocks.

Thermomagnetic analysis of MI4B (Figure 1A) reveals the presence of a single magnetic mineral with a Curie temperature of 630°C , corresponding to an oxidised (cation-deficient) magnetite.

It appears from these results that the magnetite is inhomogeneously distributed in this section of the mine and that the magnetic rocks occur in narrow bands. Thus the overall magnetisation here is probably fairly low, less than 1,000 microgauss (100 gammas), in contrast to the ECVs sampled elsewhere.

4.2 Sites 11-12

The Magazine shale is effectively non-magnetic. Natural remanent magnetisation (NRM) directions from these sites are close to the present Earth's field and may simply represent a viscous magnetisation acquired recently. However the observed directions also agree with the normal polarity directions commonly found in the Eastern Creek Volcanics and may thus be coeval with the magnetisation of the ECVs.

4.3 ECV Surface Samples

These comprise sites MI13-17, MI20 and the EV samples. In general the ECVs sampled at the surface are very magnetic, usually with remanence dominating induction.

The intensity of magnetisation is quite variable, even within a single locality, and site average values range from 2,000 to 130,000 microgauss (200-13,000 gammas) for sites 16 and 13 respectively. The picture is further complicated by the presence of two polarities (displayed in Figure 2 for sites EV1-7) of remanent magnetisation, with reversal of the remanence direction occurring in some cases on a scale of tens of metres.

The high intensities and varying polarity of remanence will produce intense local anomalies at ground level over ECV formations. However, at aeromagnetic survey heights the rapid alternation of polarities on a local scale may produce an effective cancellation of remanent magnetisation.

Thus it appears that, although detailed interpretation incorporating remanence data is not feasible due to an intractable sampling problem, interpretation may proceed by assuming the formations are magnetised by induction, at least on a gross scale.

The hypothesis that the ECVs are magnetised by induction overall depends on the assumptions that the surface samples are representative of the rock units and that both polarities of remanence are equally represented within areas of, say, 100 metres across.

The remanence of surface samples may be unrepresentative for two reasons - weathering and lightning strikes. It is believed that a number of the EV samples are lightning affected. The diagnostic signs are (i) intense but very variable NRMs, with correspondingly high Q values, and (ii) scattered NRM directions. However, lightning-induced magnetisations are magnetically softer than the thermoremanent magnetisation borne by igneous rocks, and can therefore be preferentially removed by magnetic cleaning (AF demagnetisation). Cleaning of the lightning affected samples isolates normal and reversed directions indistinguishable from those obtained elsewhere. Thus, whilst lightning may affect some of the surface rocks, application of a standard palaeomagnetic technique enables us to remove the spurious overprints and determine the remanence direction applicable to the virgin rock.

Weathering is a more insidious problem, because secondary components of magnetisation due to alteration of the magnetic minerals are often difficult to remove. The observed remanence directions, particularly after cleaning, mostly fall into two groups which are close to the present field direction and its reversed equivalent (i.e. $(0^{\circ}, -50^{\circ})$ and $(180^{\circ}, +50^{\circ})$). This is reminiscent of magnetisations acquired during Tertiary weathering. However it is considered unlikely that the observed magnetisations are associated with weathering for the following reasons

- (i) the unweathered appearance of the samples.
- (ii) the similarity of directions in the underground samples
- (iii) the high remanent intensities observed. Usually weathering destroys magnetic material and produces low intensities.

It is believed therefore that the surface samples are reasonably representative of the rock type. Normal and reversed polarities seem to be equally prevalent in most areas and should tend to cancel one another on average. Support for this conclusion can be found in the magnetic pattern over ECV units. The total field is generally higher over the volcanics than over the surrounding non-magnetic sediments, indicating that the ECVs are on the whole normally magnetised. The short wavelength

anomalies within the broad highs probably reflect alternation of remanence polarity on a local scale.

Confidence in the conclusion that the magnetisations in the ECV surface samples are not of geologically recent origin would be increased by microscopic examination of the opaques to verify that they are unaffected by weathering.

The magnetisation directions obtained from west-dipping and north-dipping sequences is similar, indicating the remanence was acquired post-folding and is therefore not a primary thermoremanent magnetisation. Any primary magnetisation was presumably reset during metamorphism of the rocks and the observed directions date from the subsequent slow cooling, which spanned several polarity intervals of the geomagnetic field. This interpretation requires considerable local inhomogeneity of the ECVs with regard to composition and grain size of the magnetic minerals, leading to a broad spectrum of blocking temperatures. The rocks with predominantly high blocking temperatures would then acquire a remanence early in the cooling, whilst rocks bearing lower blocking temperature grains would "freeze in" a magnetisation later, following one or more field reversals.

Curie point determinations reveal a range of compositions for the magnetic minerals present in the ECVs, suggesting a considerable variation in blocking temperatures. The Curie points range from 580°C (corresponding to stoichiometric magnetite) for MI13A, MI15A (Figure 1B) and MI17C, to greater than 600°C (indicating an oxidised spinel phase) for MI4B, MI13E, MI14C, MI19D, and MI15B, and down to 320°C (corresponding to pyrrhotite) for MI18D (Figure 1C). MI16C appears to have both magnetite and an unidentified phase which breaks down at about 250°C .

After taking reversed polarities into account, the mean NRM direction based on sites given in Table 3 is $(16^{\circ}, -52^{\circ})$ with an α_{95} of 20° . The corresponding pole is at 72°N , 272°E , which is consistent with an age of magnetisation around 1300-1400 m.y. The alternative is, of course, a

magnetisation associated with Tertiary weathering at about 25 m.y. However for reasons given above it is likely that the magnetisation is truly ancient.

4.4 Sites 18-19

The rock samples collected underground at these sites are fairly magnetic, in contrast to most of those from the 19 Level cross-cut. Remanence directions from the pyrrhotite-bearing MI18 samples are near randomly scattered and the effective magnetisation is likely to be predominantly induced.

The MI19 samples are much less rich in sulphides and the major magnetic carrier is magnetite. Induction dominates the remanence, which in any case is aligned sub-parallel to the Earth's field, so the overall magnetisation is along the ambient field.

Thermal and AF cleaning of specimens from these sites gives similar results to those obtained from surface samples. Originally scattered directions tend to group on cleaning about the mean normal direction or its reversed equivalent.

4.5 Urquhart Shale

Twenty-six block samples were taken over a stratigraphic thickness of several hundred metres. The samples were all very weathered and practically non-magnetic, suggesting the Urquhart shale will not make any contribution to the magnetic anomaly, at least to the bottom of the oxidised zone.

The residual remanent magnetisation directions obtained after thermal demagnetisation to 650°C (Figure 3) are well grouped around (359°, -56°) and its reverse. It is probable that the magnetisation is associated with alteration of the magnetic minerals during weathering, and the observed directions indicate an approximate average age of the weathering around 30 m.y.

5. MAGNETIC FABRIC

In an isotropic rock the induced magnetisation is always parallel to the applied field (neglecting demagnetisation effects due to specimen shape). Thus the susceptibility of the rock may be represented by a scalar quantity k , such that $\underline{M} = k\underline{H}$. In general, however, the induced magnetisation and the applied field are not strictly parallel and the susceptibility must be expressed as a tensor k_{ij} .

$$\text{Then,} \quad M_i = \sum k_{ij} H_j \quad (i, j = x, y, z)$$

The susceptibility tensor is symmetric ($k_{ij} = k_{ji}$, for all i and j) and can therefore be diagonalised. Physically, this means that three mutually perpendicular directions called the principal susceptibility axes can be found for which the magnetisation is parallel to the field. The susceptibilities along the principal axes are known as the principal susceptibilities (k_1, k_2, k_3).

We define

k_1 = major susceptibility = maximum susceptibility along any direction

k_2 = intermediate susceptibility, measured perpendicular to major and minor axes

k_3 = minor susceptibility = minimum susceptibility along any direction

k = bulk susceptibility = $(k_1+k_2+k_3)/3$

A = susceptibility anisotropy = $k_1/k_3 > 1$

P = prolateness = $(k_1-k_2)/(k_2-k_3)$

For most rocks the anisotropy is small ($A \approx 1$) and the susceptibility along any direction is close to the bulk susceptibility. The maximum possible deflection of the induced magnetisation towards the easiest direction of magnetisation (the major susceptibility axis) is given by

$$\theta = \tan^{-1} [(A-1)/2\sqrt{A}]$$

For example, in the worst possible case, for 50% anisotropy ($A = 1.5$) the deflection of the induced magnetisation away from the applied field is 12° .

The origin of the susceptibility anisotropy depends on the magnetic minerals present in the rock. The most common causes of magnetic anisotropy in rocks are

- (i) Alignment of the long axes of inequidimensional magnetic grains. The anisotropy arises from self-demagnetising effects on the grains (shape anisotropy).
- (ii) Alignment of the C-axes of haematite or pyrrhotite crystals. These minerals exhibit strong magnetocrystalline anisotropy with an easy plane of magnetisation (the basal plane). The susceptibility along the C-axis is much lower than in the basal plane.
- (iii) Textural anisotropy arising from concentration of strongly magnetic grains (magnetite or pyrrhotite) into strings or planes. As in (i) the anisotropy arises from self-demagnetisation. A good example of this type of anisotropy is afforded by banded iron formations for which the susceptibility in the bedding plane is much greater than that normal to the bedding.

The major and intermediate susceptibility axes define a maximum susceptibility plane, which has a pole coinciding with the minimum susceptibility axis. The simplest interpretation of the susceptibility anisotropy is then to regard the maximum susceptibility plane as a foliation, within which there is a lineation corresponding to the major susceptibility axis. Obviously the foliation plane can be defined by the foliation pole given by the minimum susceptibility axis.

.. The magnetic fabric defined in this way usually corresponds well with any visible rock fabric present. In addition, a definite magnetic fabric

is found in most rocks although they may exhibit no visible petrofabric. Thus susceptibility anisotropy measurements are potential aids to structural interpretation based on rock fabric studies, and appear to be a rapid and reliable alternative to tedious and time-consuming petrographic techniques.

Care must be taken, however, in the interpretation of magnetic fabrics as there is an inherent ambiguity associated with overprinted fabrics. For instance, two non-parallel foliations will be expressed magnetically as a single foliation lying between the two planes, with a lineation along the intersection of the planes. A lineation oblique to a foliation plane will appear as a foliation lying between the true lineation and foliation plane, containing a lineation along the projection of the true lineation onto the apparent foliation plane. Thus rock fabrics of low symmetry will find their expression in a magnetic fabric of higher symmetry, and some information will be lost. In practice, this limitation is usually not serious.

In unaltered sediments the magnetic fabric is usually bedding-parallel and the lineation reflects the palaeocurrent direction. Deformation aligns the lineation with the fold axis. Low grade metasediments tend to retain a bedding-parallel planar fabric, but highly metamorphosed rocks usually possess a purely deformational magnetic fabric.

The most notable feature of the data in Table 4 is the consistency of foliation pole directions from all the samples listed. Apart from a couple of slightly anomalous directions, probably reflecting small-scale folds, the poles have moderate to shallow plunge to the east. The mean foliation pole from all samples is (88° , $+22^{\circ}$) with an error of 8° , i.e. the average foliation plane is dipping at about 70° to the west - parallel to the bedding around Mt Isa. Slight local variations of this dip are apparent. For instance the mean foliation pole from sites 1-10 (5262 mN cross-cut) is (87° , $+37^{\circ}$) ($\alpha_{95} = 21^{\circ}$) indicating a westerly dip of about 50° . At locality 18 the magnetic foliation is

parallel to the visible banding of sulphides in the rock. This suggests that the magnetic fabric arises from textural anisotropy of pyrrhotite layers, in this part of the mine.

For most of the samples $P < 1$, that is the fabric is predominantly planar. However the major and intermediate susceptibility axes are far from randomly oriented within the foliation plane. In most cases the maximum susceptibility direction is well defined within samples, as indicated by the low errors on the lineation directions. Lineation directions are variable, however, from locality to locality, and overall are strung along the great circle representing the regional foliation plane. Overall the lineations range from NW plunging to SW plunging, with steep westerly plunges predominating.

If petrographic work in the mine area reveals a linear fabric coinciding with the magnetic lineations in the mine samples, the present results would enable extrapolation of the petrofabric interpretation to the other sampling localities.

Susceptibility anisotropy will not significantly affect the direction of magnetisation of these rocks and can be ignored for magnetic interpretation. This follows from the relatively low values of anisotropy, the fact that the present Earth's field lies close to the plane of maximum susceptibility, and the prevalence of high Q values implying that induction is only a minor component of the total magnetisation.

6. CONCLUSIONS

1. The Eastern Creek Volcanics are overall very magnetic and are usually intensely remanently magnetised.

Normal and reversed polarities of remanent magnetisation occur ubiquitously, and seem to be equally common.

It is therefore suggested that the average magnetisation of the ECV units is due to induction alone, with remanent magnetisation responsible for the small wavelength anomalies apparent from the complexity of the magnetic signature over the ECVs.

A guide to the average magnetisation of the various rock units should then be provided by the susceptibility values given in Table 2.

2. Application of palaeomagnetic cleaning techniques and comparison with results from underground sampling have increased confidence that the surface samples are representative of the bulk of the sampled lithology, and that surface effects are not masking the true average remanence direction.

The remanent magnetisation of the ECVs is believed to be associated with the regional metamorphism of the area.

3. Anisotropy of susceptibility in the ECVs is negligible for the purpose of magnetic interpretation, however the presence of a well defined magnetic fabric in these rocks may allow application of susceptibility anisotropy measurements to structural interpretation. In the area around Mt Isa the magnetic foliations consistently dip steeply to the west, parallel to the bedding. Magnetic lineations are also present and have steep NW to SW plunges.

TABLE 1. SAMPLING LOCALITIES

	Rock type	Locality
SITES 1-10	Eastern Creek Volcanics in mine	5262 mN cross-cut at 19 level
SITE 11	Magazine Shale	42,200 mN; 10,900 mE
SITE 12	Magazine Shale	42,300 mN; 10,900 mE
SITE 13	Pickwick Beds	30,100 mN; 11,100 mE
SITE 14	Cromwell Beds	29,800 mN; 12,100 mE
SITE 15	ECVs west of Judenan Beds	38,600 mN; 8,800 mE
SITE 16	ECVs west of Doolan's Hope	43,200 mN; 10,700 mE
SITE 17	Cromwell Beds	23,200 mN; 16,400 mE
SITE 18	ECVs in mine	13 level, 4805 cross-cut
SITE 19	ECVs in mine	15 level, 6461 cross-cut
SITE 20	Paroo Beds	34,200 mN; 11,200 mE

Previously sampled:

IS1-26 [†]	Urquhart Shale	Mine area, 4,300mN; 1,400mE
EV1-6,28-33 [*]	ECVs	Microwave tower - Breakaway creek (37,500 mN; 20,350 mE - 36,400 mN; 16,250 mE)
EV7 [*]	ECVs	West of Dajarra
EV8-17 [*]	ECVs	Mt Isa-Gunpowder road (139°25'E, 19°45'S-139°25'E, 19°52'S)
EV18-27 [*]	ECVs	139°35'E, 20°S

† samples * sites

TABLE 2. SUSCEPTIBILITY AND REMANENT INTENSITY

Sample No.	N	\bar{k} (Range or \pm SE)	\bar{J} (Range or \pm SE)	\bar{Q} (Range or \pm SE)
1	14	52 \pm 2	1 (0-7)	0.03 (0.00-0.08)
2	4	45 \pm 5	0.5 \pm 0.1	0.02 (0.01-0.03)
3A	8	30 \pm 1	0.2 \pm 0.06	0.02 \pm 0.003
3B	5	64 \pm 1	0.3 (0.2-0.6)	0.01 \pm 0.002
4A	13	48 \pm 1	1.0 \pm 0.1	0.04 \pm 0.003
4B	7	4,000 \pm 300	330 \pm 40	0.16 \pm 0.01
5	6	43 \pm 1	0.6 \pm 0.1	0.03 \pm 0.003
6	4	63 \pm 4	2.1 \pm 0.3	0.07 \pm 0.006
7	7	54 \pm 1	1.3 \pm 0.2	0.05 \pm 0.007
8	5	5,800 \pm 1700	290 (30-650)	0.08 \pm 0.01
9	8	63 \pm 13	1.1 (0.3-1.4)	0.03 \pm 0.005
10	11	88 \pm 3	2.7 \pm 0.2	0.06 \pm 0.006
11A-F	18	25 \pm 2	30 (1-200)	2.2 (0.0-11.2)
12A-D	5	11 \pm 1	5 (1-10)	0.9 (0.2-1.8)
13A-D	12	14,000 \pm 2,000	64,000 \pm 17,000	7.5 \pm 1.4
13E-F	3	11,700 \pm 1,100	197,000 (132,000-278,000)	33 \pm 6
14A	8	9,700 \pm 300	41,000 \pm 5,000	8.5 \pm 1.3
14B	15	6,200 \pm 500	3,400 \pm 300	1.09 \pm 0.02
14C	9	15,600 \pm 700	21,800 \pm 1,300	2.73 \pm 0.05
15A	13	8,350 \pm 120	13,300 \pm 600	3.1 \pm 0.1
15B	11	5,700 \pm 200	3,100 \pm 200	1.07 \pm 0.09
15C	14	10,000 \pm 300	4,900 \pm 400	1.0 \pm 0.1
16A	10	4,800 \pm 200	2,300 \pm 100	0.94 \pm 0.02
16B	18	750 \pm 50	125 \pm 9	0.35 \pm 0.03

Table 2. (continued)

Sample No.	N	\bar{k} (Range or \pm SE)	\bar{J} (Range or \pm SE)	\bar{Q} (Range or \pm SE)
16C	4	1,900 \pm 300	420 \pm 40	0.5 \pm 0.1
17A	6	14,800 \pm 500	84,000 \pm 5,000	11.1 \pm 0.3
17B	16	19,000 \pm 1,000	172,000 \pm 19,000	18 \pm 2
17C	4	12,800 \pm 300	30,000 \pm 5,000	4.6 \pm 0.6
18A	3	2,100 \pm 200	1,400 \pm 200	1.3 \pm 0.1
18B	24	730 \pm 70	260 \pm 40	0.69 \pm 0.09
18C	8	760 \pm 200	340 \pm 120	1.28 \pm 0.06
18D	10	2,100 \pm 300	900 \pm 200	0.9 \pm 0.2
18E	12	1,200 \pm 200	630 \pm 80	1.2 \pm 0.2
19A	7	3,200 \pm 700	230 (80-540)	0.13 \pm 0.02
19B	10	14,900 \pm 600	1,750 \pm 100	0.23 \pm 0.01
19C	12	5,800 \pm 500	430 \pm 50	0.15 \pm 0.01
19D	3	12,700 \pm 1,500	2,650 \pm 250	0.41 \pm 0.03
19E	7	3,000 (920-9,550)	170 (30-620)	0.12 \pm 0.02
20A	9	10 \pm 1	0.9 \pm 0.2	0.17 \pm 0.02
IS1-26		<100	0-500	-
EV1-6*		-	\sim 10,000	-
EV7*		-	1,200 (300-2,800)	-
EV8-17*		\sim 5,000	\sim 50,000	\sim 20
EV18-27*		\sim 4,000	\sim 500	\sim 0.25
EV28-33*		-	\sim 1,800	-

N = no. of specimens, k = emu susceptibility $\times 10^6$, J = NRM intensity in microgauss, Q = J/kH where H = 0.51 Oersteds

Averages are arithmetic means. The standard error of the mean is given if the dispersion of values is low enough to make this meaningful, otherwise the range of values is quoted.

* sites, comprising 4 to 26 samples each.

TABLE 3. REMANENCE DIRECTIONS

	Mean NRM Direction (α_{95})	
SITES 1-10	Directions very scattered, but normal directions predominate	
SITES 11-12	(10°, -50°)	(8°)
MI13A-D	(180°, +53°)	(44°)
MI13E-F	(32°, -49°)	(24°)
MI14A	(186°, +62°)	(9°)
MI14B	(27°, -44°)	(5°)
MI14C	(14°, -24°)	(2°)
MI15A	(246°, +66°)	(2°)
MI15B	(350°, -68°)	(4°)
MI15C	(297°, +55°)	(6°)
MI16A-C	(314°, -55°)	(18°)
MI17A	(215°, +15°)	(6°)
MI17B	(304°, +33°)	(12°)
MI17C	(120°, +3°)	(4°)
MI18	Directions very scattered but predominantly reversed	
MI19	(14°, -51°)	(26°)
MI20A	(279°, +16°)	(51°)
IS1-26	Scattered, predominantly normal directions	
EV1-6	Scattered normal and reversed directions with normal predominating	
EV7	Normal	
EV8-17	Very scattered normal and reversed directions	
EV18-27	"	" " "
EV28-33	Scattered, predominantly normal directions	

Directions are quoted in the form (declination, inclination) where declination is positive clockwise from north, inclination is positive downwards. The mean directions are based on unit weight to specimens

α_{95} = semi-angle of the 95% confidence cone about the mean direction

TABLE 4. MAGNETIC FABRIC

Sample No.	Anisotropy (Range or \pm SE)	Fabric Type	Foliation pole (α_{95})	Lineatic (α_{95})
1	1.03 \pm 0.01	P \approx 1	(93°, 56°) (13°)	(320°, 27°) (12°)
2	1.09 \pm 0.01	P<1	(136°, 60°) (27°)	(263°, 18°) (19°)
3A	1.01 \pm 0.002	P \approx 1	(0°, 34°) (5°)	(199°, 55°) (9°)
3B	1.08 \pm 0.02	P<1	(94°, 63°) (5°)	(283°, 27°) (8°)
4A	1.025 \pm 0.007	P<1	(111°, 40°) (5°)	(387°, 35°) (27°)
4B	1.20 \pm 0.006	P<1	(111°, 36°) (5°)	(334°, 43°) (27°)
5	1.007 \pm 0.007	P \approx 1	(81°, 25°) (14°)	(250°, 65°) (14°)
6	1.02 \pm 0.01	P<1	(76°, 30°) (11°)	(273°, 57°) (33°)
7	1.07 \pm 0.02	P<1	(71°, 25°) (5°)	(326°, 28°) (26°)
8	1.24 \pm 0.015	P<1	(90°, -30°) (6°)	(315°, 51°) (7°)
9	1.10 \pm 0.04	P<1	(83°, -40°) (9°)	(294°, -48°) (25°)
10	1.04 \pm 0.006	P<1	(99°, 22°) (6°)	(344°, 41°) (15°)
11A-F	1.14 \pm 0.05	P<1	(92°, 13°) (9°)	(234°, 74°) (10°)
12A-D	1.13 \pm 0.06	P>1	(93°, 14°) (27°)	(233°, 70°) (9°)
13A-F	1.14 \pm 0.01	P \approx 1	(117°, 18°) (7°)	(236°, 57°) (11°)
14A	1.05 \pm 0.005	P<1	(86°, 11°) (11°)	(185°, 31°) (10°)
14B	1.07 \pm 0.003	P<1	(94°, 25°) (7°)	(206°, 37°) (11°)
14C	1.04 \pm 0.002	P<1	(93°, 13°) (6°)	(201°, 53°) (9°)
15A	1.70 \pm 0.006	P>1	(77°, 21°) (1°)	(302°, 62°) (1°)
15B	1.33 \pm 0.005	P>1	(72°, 1°) (3°)	(308°, 88°) (5°)
15C	1.54 \pm 0.01	P>1	(80°, 5°) (2°)	(324°, 79°) (2°)

Sample No.	Anisotropy (Range or \pm SE)	Fabric Type	Foliation pole (α_{95})	Lineation (α_{95})
16A	1.16 \pm 0.01	P<1	(80°, 6°) (5°)	(193°, 76°) (4°)
16B	1.12 \pm 0.006	P _v 1	(96°, 12°) (10°)	(213°, 68°) (5°)
16C	1.12 \pm 0.01	P _v 1	(93°, 22°) (7°)	(240°, 65°) (9°)
17A	1.147 \pm 0.002	P>1	(99°, 5°) (5°)	(230°, 83°) (6°)
17B	1.18 \pm 0.01	P _v 1	(103°, 11°) (3°)	(230°, 72°) (2°)
17C	1.10 \pm 0.006	P _v 1	(93°, 6°) (6°)	(214°, 79°) (3°)
18A	1.33 \pm 0.09	P<1	(86°, 21°) (10°)	(179°, 7°) (66°)
18B	1.44 \pm 0.02	P>1	(72°, 15°) (5°)	(298°, 69°) (3°)
18C	1.28 \pm 0.06	P>1	(64°, -24°) (24°)	(353°, 37°) (13°)
18D	1.66 \pm 0.07	P>1	(77°, 12°) (9°)	(288°, 76°) (6°)
18E	1.41 \pm 0.04	P _v 1	(62°, 17°) (8°)	(310°, 54°) (9°)
19A	1.10 \pm 0.01	P<1	(122°, 26°) (13°)	(231°, 30°) (17°)
19B	1.15 \pm 0.01	P<1	(89°, 27°) (19°)	(351°, 11°) (12°)
19C	1.15 \pm 0.01	P<1	(106°, 20°) (4°)	(200°, 10°) (4°)
19D	1.21 \pm 0.01	P<1	(113°, 15°) (34°)	(209°, 22°) (20°)
19E	1.20 \pm 0.03	P<1	(108°, 59°) (22°)	(197°, 9°) (29°)
20A	1.03 \pm 0.01	P _v 1	(40°, 24°) (34°)	(293°, 44°) (26°)

k_1 = susceptibility measured along easiest direction of magnetisation (major susceptibility axis)

k_2 = intermediate susceptibility (measured perpendicular to major and minor susceptibility axes)

k_3 = susceptibility measured along hardest direction of magnetisation (minor susceptibility axis)

$$k_1 \geq k_2 \geq k_3$$

$$\text{Anisotropy} = k_1/k_3$$

$$\text{Prolateness } P = (k_1 - k_2)/(k_2 - k_3)$$

P>1 signifies lineation more pronounced than foliation (linear fabric)

P<1 signifies foliation more pronounced than lineation (planar fabric).

The foliation pole is the mean of the minor susceptibility axis directions.

The lineation direction is the mean of the major susceptibility axis directions.

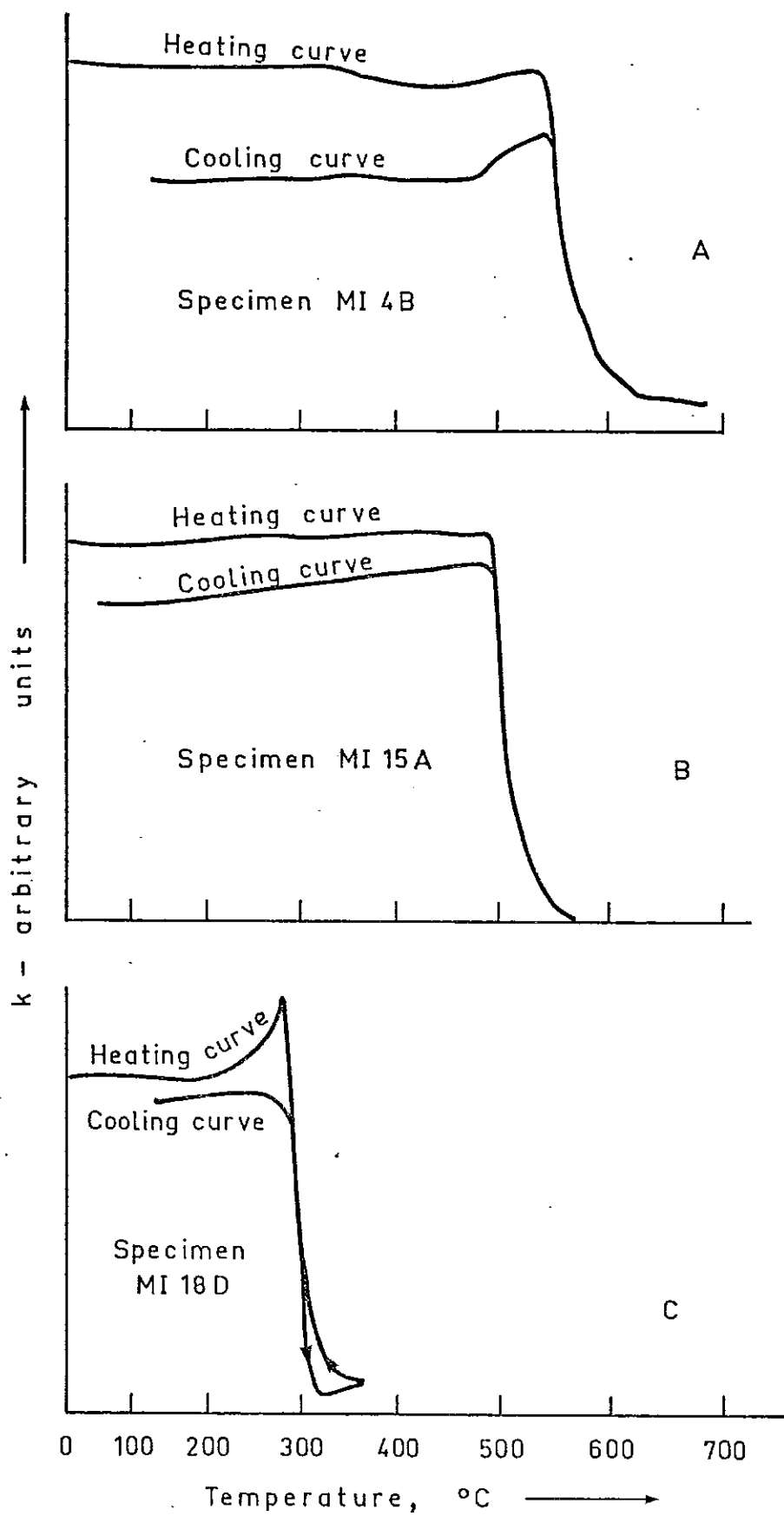


FIG. 1

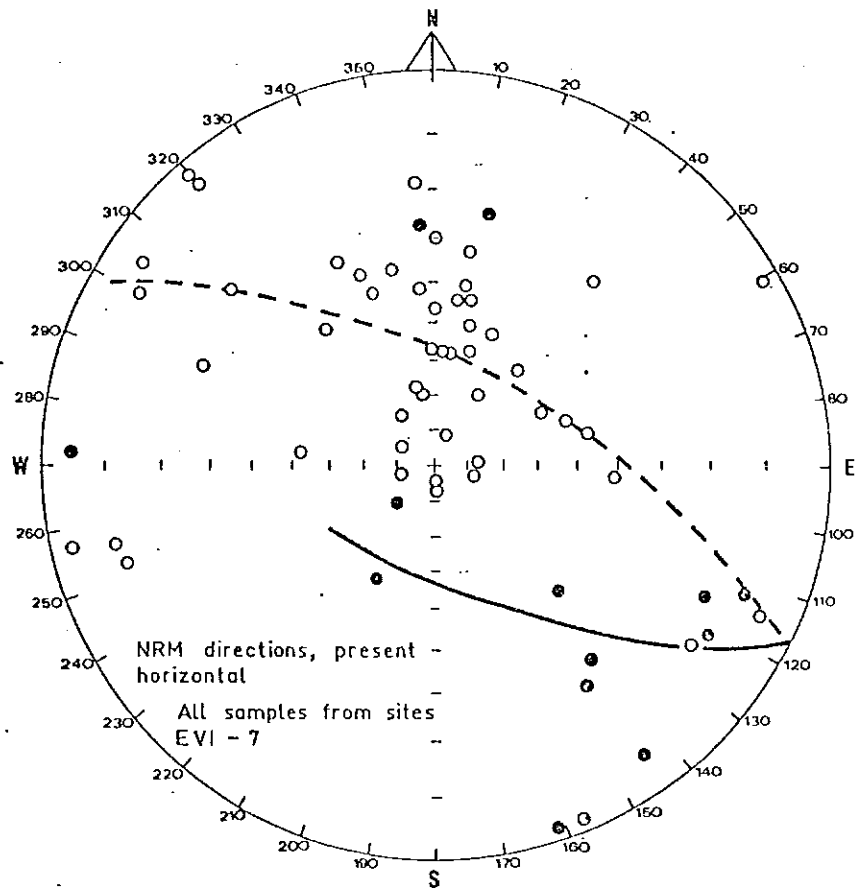


FIG. 2A

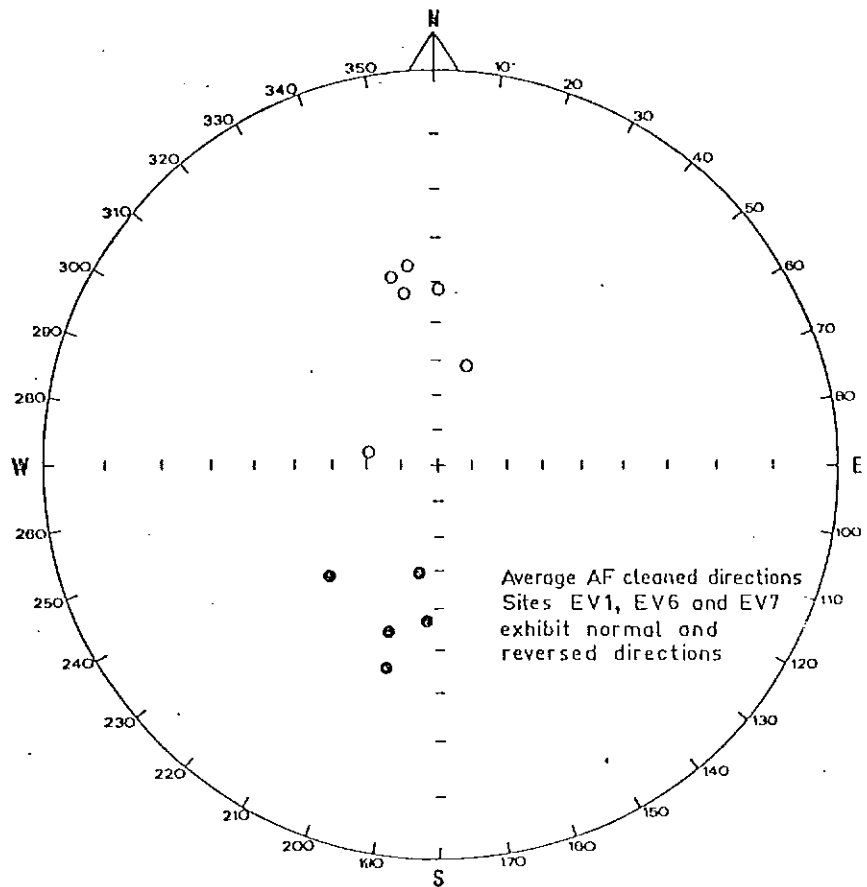


FIG. 2B

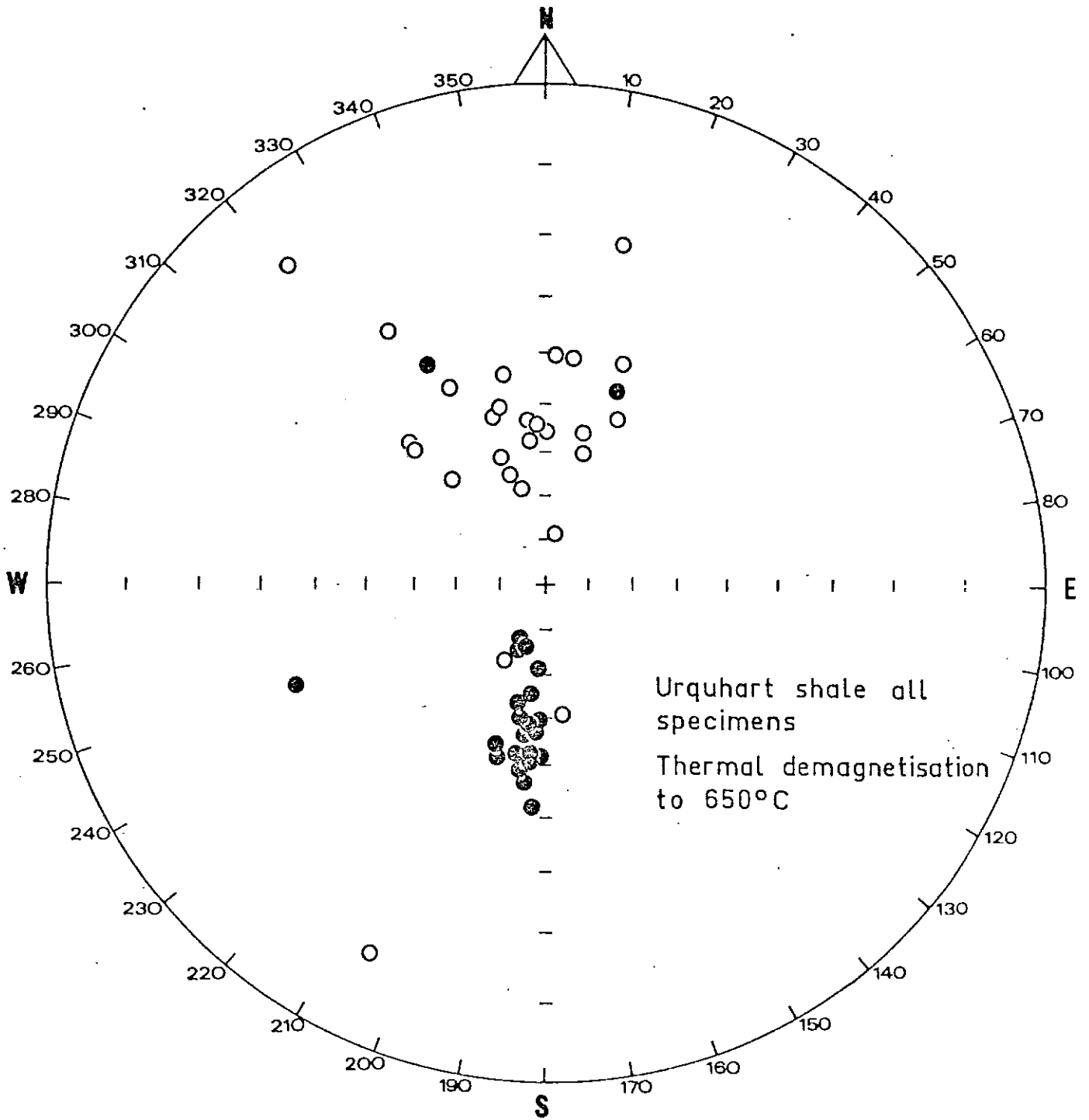


FIG. 3